Acceleration of the methanolysis of phosphate diesters promoted by $La(OTf)_3$ — The analysis of non-integer $^{s}_{s}$pH/rate profiles resulting from changes in metal ion speciation[1]

Graham T.T. Gibson, Alexei A. Neverov, Allen Chun-Tien Teng, and R.S. Brown

Abstract: In a previous publication (A.A. Neverov and R.S. Brown. Inorg. Chem. **40**, 3588 (2001)) we reported very effective catalysis of the methanolysis of some phosphate diesters (methyl *p*-nitrophenyl phosphate (**1**), bis(*p*-nitrophenyl) phosphate (**2**), and diphenyl phosphate (**3**)) promoted by La^{3+}, and noted a general observation that the plots of $\log k_{cat}$ vs. $^{s}_{s}$pH had non-integer gradients. In this report the origins of that behaviour are studied and analyzed through determination of the speciation of $La^{3+}(^{-}OCH_3)_n$, $(La^{3+})_2(^{-}OCH_3)_m$, $(La^{3+})_2$:phosphate:$(^{-}OCH_3)_y$ forms in solution as a function of $^{s}_{s}$pH. Potentiometric titrations of solutions of $La(OTf)_3$ in methanol at low ($<1 \times 10^{-4}$ mol/L) and high ($>1 \times 10^{-3}$ mol/L) concentration were analyzed through fits of the data to various models to provide speciation diagrams of the various La^{3+} forms in the absence of phosphate. Titrations of La^{3+} in the presence of diphenyl phosphate were also analyzed to provide speciation diagrams for phosphate bound forms. The kinetic data for the La^{3+} catalyzed methanolysis of **1** were analyzed through fitting the kinetic data at low and high $[La^{3+}]$ as a function of $^{s}_{s}$pH to a linear combination of the individual kinetic contributions of each species. Overall the data are best analyzed in the low $[La^{3+}]$ domain as resulting from methoxide attack on a transient complex of phosphate bound to $La^{3+}(^{-}OCH_3)_{0,1}$. In the high $[La^{3+}]$ domain the data fit two kinetically equivalent processes involving either a spontaneous decomposition of $(La^{3+})_2$:**1**$^{-}$:$(^{-}OCH_3)_{2,3,4,5}$ or external methoxide attack on $(La^{3+})_2$:**1**$^{-}$:$(^{-}OCH_3)_{1,2,3,4}$.

Key words: lanthanides, phosphate diester, methanolysis, kinetics, speciation, metal ion catalysis of methanolysis, DNA model methanolysis.

Résumé : Dans une publication antérieure (A.A. Neverov et R.S. Brown. Inorg. Chem. **40**, 3588 (2001)), nous avons rapporté une catalyse très efficace de la méthanolyse de quelques esters de l'acide phosphorique (phosphate de méthyle et de *p*-nitrophényle (**1**), phosphate de bis(*p*-nitrophényle) (**2**) et phosphate de diphényle (**3**)) sous l'influence du La^{3+} et nous avons noté que les gradients des courbes du $\log k_{cat}$ vs. $^{s}_{s}$pH n'étaient pas des nombres entiers. Dans ce travail, nous avons étudié ce comportement et l'avons analysé par une détermination de la spéciation des formes $La^{3+}(^{-}OCH_3)_n$, $(La^{3+})_2(^{-}OCH_3)_m$ et $(La^{3+})_2$:phosphate:$(^{-}OCH_3)_y$ en solution en fonction du $^{s}_{s}$pH. Afin de pouvoir obtenir des diagrammes de spéciation des diverses formes de La^{3+} en l'absence de phosphate, nous avons analysé les résultats de titrages potentiométriques de solutions de $La(OTf)_3$ dans le méthanol, à des concentrations basses ($<1 \times 10^{-4}$ mol/L) et élevées ($>1 \times 10^{-3}$ mol/L), en procédant à divers ajustements des données à divers modèles. Afin d'obtenir des diagrammes de spéciation des formes liées du phosphate, nous avons aussi analysé les données des titrages du La^{3+} en présence de phosphate de diphényle. Les données cinétiques pour la méthanolyse du **1** catalysée par le La^{3+} ont été analysées par le biais d'un ajustement des données à des concentrations faibles et élevées de La^{3+} en fonction de $^{s}_{s}$pH afin d'obtenir une combinaison linéaire des contributions cinétiques individuelles de chaque espèce. Dans l'ensemble, la meilleure façon d'expliquer les données dans le domaine de faible concentration de La^{3+} implique une attaque du méthanolate sur un phosphate intermédiaire lié à un $La^{3+}(^{-}OCH_3)_{0,1}$. Dans le domaine de concentration élevée de La^{3+}, les données peuvent être expliquées par deux processus cinétiquement équivalents impliquant soit une décomposition spontanée d'un complexe $(La^{3+})_2$:**1**$^{-}$:$(^{-}OCH_3)_{2,3,4,5}$ ou une attaque externe d'un méthanolate sur un complexe $(La^{3+})_2$:**1**$^{-}$:$(^{-}OCH_3)_{1,2,3,4}$.

Mots clés : lanthanides, diester de l'acide phosphorique, méthanolyse, cinétique, spéciation, catalyse par un ion métallique d'une méthanolyse, méthanolyse modèle de l'ADN.

[Traduit par la Rédaction]

Received 12 December 2004. Published on the NRC Research Press Web site at http://canjchem.nrc.ca on 18 October 2005.

G.T.T. Gibson, A.A. Neverov, A.C.-T. Teng, and R.S. Brown.[2] Department of Chemistry, Queen's University, Kingston, ON K7L 3N6, Canada.

[1]This article is part of a Special Issue dedicated to organic reaction mechanisms.
[2]Corresponding author (e-mail: rsbrown@chem.queensu.ca).

 doi: 10.1139/V05-065

Introduction

Various studies from these labs have shown that La^{3+}, along with 1 equiv. of methoxide in methanol, is an extraordinarily active catalyst for the methanolysis of carboxylate esters (1), β-lactams (2), and a variety of phosphates and thiophosphates including phosphate di- and triesters (3). The phosphate diester linkage is biologically important because it is ideal for preserving genetic information in RNA and DNA because of its kinetic robustness toward hydrolysis. To facilitate what is otherwise a very slow hydrolytic process, Nature provides various metallo-enzymes (4) such as the RNAse from HIV reverse transcriptase (4*a*), 3′–5′ exonuclease from DNA polymerase I (4*b*), and P1 nuclease (4*c*) to cleave phosphate diesters so it is not surprising that a large number of studies have been reported concerning metal-ion-promoted hydrolysis of $(RO)(R'O)PO_2^-$ species (5).

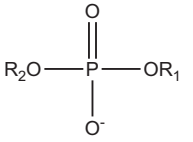

1 $R_2O = OCH_3$, $R_1O = OC_6H_4NO_2$
2 $R_2O = R_1O = OC_6H_4NO_2$
3 $R_2O = R_1O = OC_6H_5$

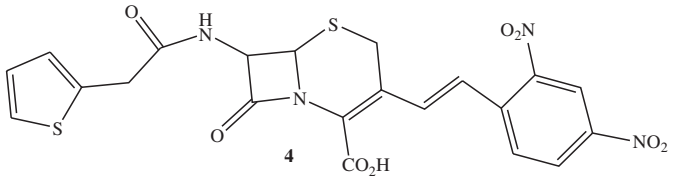

4

Interestingly, metal-catalyzed alcoholysis of phosphate diesters is, to our knowledge, a scarcely investigated area although our own studies (3*a*) showed that the methanolyses of methyl *p*-nitrophenyl phosphate (**1**), bis(*p*-nitrophenyl) phosphate (**2**), and diphenyl phosphate (**3**) were accelerated by as much as 10^{10}-fold in the presence of La^{3+} compared to the background methoxide promoted reaction. Unfortunately, a comprehensive mathematical fit of the kinetic behaviour to a given mechanism that included all the species responsible for catalysis as a function of $^{s}_{s}$pH was not possible due to the complexity of the situation as revealed from kinetic plots of the observed pseudo-first-order rate constant (k_{obs}) for the methanolysis of **1** as a function of $[La^{3+}]$ at various $^{s}_{s}$pH values. Typically, the plots show (3*a*) two $^{s}_{s}$pH-dependent domains of interest, which are illustrated schematically in Fig. 1 (see Figs. 1S and 2S, Supplementary material, for the appearance of these plots at two different $^{s}_{s}$pH values).[3] On the basis of these plots, we rationalized the kinetic behaviour in terms of the simplified process given in Scheme 1, where monomeric and dimeric forms of La^{3+} associated with variable numbers of methoxides in a $^{s}_{s}$pH-dependent way were responsible for the catalysis.

Fig. 1. Plot of pseudo-first-order rate constants for the methanolysis of **1** (2×10^{-5} mol/L) vs. $[La(OTf)_3]$ at 25 °C; $^{s}_{s}$pH = 11.1 (0.02 mol/L triethylamine buffer). Based on data from ref. 3*a*. The values of $k_2^{\mathbf{1}}$ and $k_1^{\mathbf{1}}$ are taken as the limiting plateau value and initial gradient of the plots at given $^{s}_{s}$pH values; double-headed arrows show the direction of change of $k_2^{\mathbf{1}}$ and $k_1^{\mathbf{1}}$ as a function of $^{s}_{s}$pH.

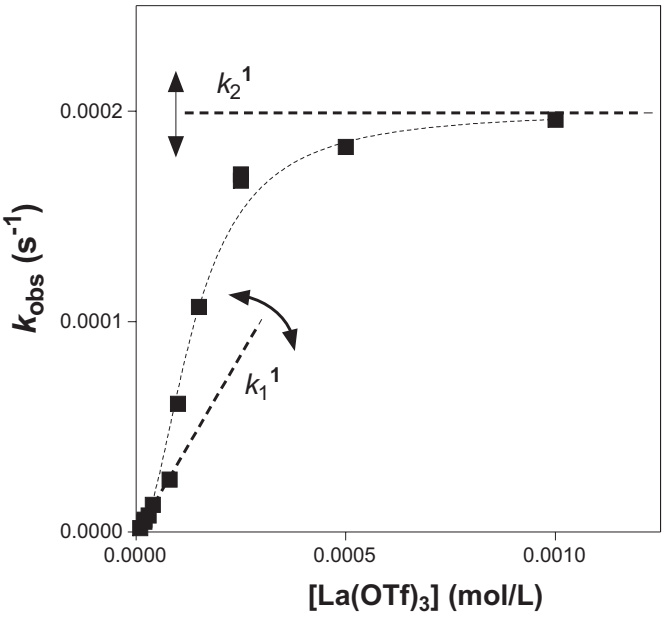

Scheme 1.

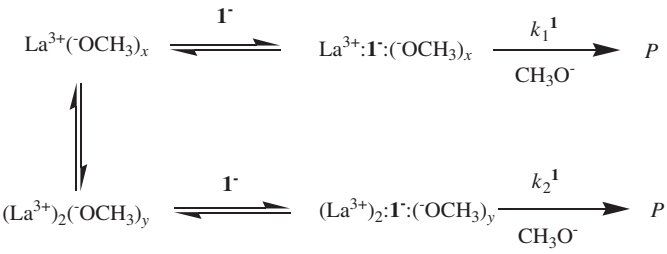

At limiting low and high $[La^{3+}]$ we could define the $k_1^{\mathbf{1}}$ and $k_2^{\mathbf{1}}$ as the slope and plateau, respectively, of the k_{obs} vs. $[La^{3+}]$ plots at each $^{s}_{s}$pH, the values being reproduced in Table 1S of the Supplemental material.[3] Curiously, neither $k_1^{\mathbf{1}}$ nor $k_2^{\mathbf{1}}$ shows a unit linear dependence on $[^{-}OCH_3]$, the slopes being 0.35 and 0.5, respectively (3*a*): in the case of the $k_1^{\mathbf{1}}$ plot there is a serious downturn at the highest $^{s}_{s}$pH values.

Typically, log plots of rate constant vs. [lyate], [lyoxide], [catalyst], or $[M^{x+}]$ have integer gradients of 0, 1, or 2, which result from rate-limiting processes having zero-, first-, or second-order dependencies on the concentration of the species of interest. In some common cases such kinetic plots exhibit "saturation" behaviour, with a domain of unit slope evolving into a plateau of zero slope at higher concentration indicative of a substrate associated with the catalytic entity in a kinetically competent 1:1 complex. Non-integer kinetic

[3] Supplementary data for this article are available on the Web site or may be purchased from the Depository of Unpublished Data, Document Delivery, CISTI, National Research Council Canada, Ottawa, ON K1A 0S2, Canada. DUD 4014. For more information on obtaining material refer to http://cisti-icist.nrc-cnrc.gc.ca/irm/unpub_e.shtml.

plots are far less common for ionic reactions[4] (6) although square root dependencies are often observed for reactions catalyzed by metal ions that dimerize to inactive forms such as was found in our recent study of the Zn^{2+} promoted methanolysis of *p*-nitrophenyl acetate and the phosphate triester paraoxon (7), or the Cu^{2+} catalyzed hydrolysis of *p*-nitrophenyl diethyl phosphate (8).

In cases where the speciation of a M^{x+} catalyst changes as a function of its concentration or as a function of pH, one can envision an alteration of the catalytic properties in such a way that the pH / log rate constant profiles can have non-integer gradients or exhibit irregular upward or downward curvature. This phenomenon is probably a general one, the recognition and incorporation of which will prove particularly applicable to studies of mono- and polymetal ion catalysis as a function of pH where the pH / log rate constant profiles do not vary in a regular way (9). Indeed, in a recent analysis of the La^{3+} promoted methanolysis of the β-lactam nitrocefin (**4**) we demonstrated (2) that the nonunit slope for the kinetic data as a function of ${}^{s}_{s}$pH could be accommodated by two kinetically equivalent mechanisms: methoxide attack on $La^{3+}{}_2(\mathbf{4}^-)(^-OCH_3)_n$, n = 0–2, or spontaneous decomposition of the forms $La^{3+}{}_2(\mathbf{4}^-)(^-OCH_3)_n$, n = 1–3.

In this report we analyze the previously obtained rate data for the La^{3+} catalyzed methanolysis of **1** (3*a*) in terms of models involving La^{3+} monomers and dimers with varying numbers of methoxides, the speciation of which depends upon [La^{3+}] concentration and the ${}^{s}_{s}$pH. The speciation of La^{3+} at low (<2 × 10^{-4} mol/L) and high (>1 × 10^{-3} mol/L) metal ion concentrations is computed through analysis of the potentiometric titration data using the program Hyperquad 2000 (10). At high concentrations of metal ion, where the kinetics are suggestive of the formation of $La^{3+}{}_2$ bound phosphate, we have conducted the titrations on solutions of La^{3+} with a fixed 2:1 La^{3+} : diphenyl phosphate ratio, analyzing these to determine the metal ion binding constants and speciation. Finally, we have analyzed the kinetic data in terms of the contributions of the various species present in solution to develop an internally consistent explanation of the shapes of the ${}^{s}_{s}$pH/rate profiles.

Experimental

Materials

Methanol (anhydrous, 99.8%), sodium methoxide (0.5 mol/L in MeOH), lanthanum trifluoromethanesulfonate (99.999%), bis(*p*-nitrophenyl) phosphate (**2**, 99%), and diphenyl phosphate (**3**, 99%) were all purchased from Aldrich and used without any further purification.

${}^{s}_{s}$pH Measurements

The $CH_3OH_2^+$ concentration was determined for kinetic and titration measurements using a Radiometer pHC4000-8 or an Accumet model 13-620-292 combination glass electrode calibrated with Fisher certified standard aqueous buffers (pH = 4.00 and 10.00) as described in our recent papers (11). Values of ${}^{s}_{s}$pH were calculated by subtracting a correction constant of –2.24 from the experimental meter reading (${}^{s}_{w}$pH). This method was described by Bates and co-workers (12*b*, 12*c*) for a molality scale (correction constant –2.34) and later by Bosch and co-workers (13) for a molar correction constant of –2.24 units.

${}^{s}_{s}p\mathit{K}_a$ Determination

The potentiometric titrations of $La(OTf)_3$ and diphenyl phosphate in methanol were performed using a Metrohm model 798 Titrino automatic titrator under anaerobic conditions (Ar) at 25.0 ± 0.1 °C. Methanolic $La(OTf)_3$ and diphenyl phosphate stock solutions (0.02 or 0.002 mol/L) were diluted to the required concentrations by adding anhydrous methanol. The total sample volume in all cases was 20.0 mL. Sodium methoxide titrant, prepared from stock 0.5 mol/L $NaOCH_3$ in a Sure Seal® bottle, was 0.021 or 0.0028 mol/L and was calibrated by titrating Fisher certified standard HCl in water, with the endpoint taken to be ${}^{w}_{w}$pH 7. After each titration the electrode was immersed in pH 4.00 aqueous buffer or a dilute aq. HCl solution for several minutes. The electrode was then rinsed with MeOH, dried with a tissue, and used for the next titration. The electrode was recalibrated often to ensure accurate readings.

The values of the species formation constants in methanol were calculated using the computer program Hyperquad 2000 (version 2.1 NT) (10), with the autoprotolysis constant of pure methanol taken to be $10^{-16.77}$ (13) at 25 °C. The formation constants for the species $La^{3+}{}_2(^-OMe)_n$ (n = 1–5) were determined from the analysis of the potentiometric titration of 1 × 10^{-3} mol/L $La(OTf)_3$. Two such titrations were analyzed separately and their respective species formation constants averaged; the resulting values were used as constants in the subsequent Hyperquad analysis of 2:1 $La(OTf)_3$:phosphate titrations. Similarly, formation constants for the species $La^{3+}(^-OMe)_n$ (n = 1–3) were determined from the analysis of the titration of 1 × 10^{-4} mol/L $La(OTf)_3$. Because the methanolysis of phosphates **1** and **2** in the presence of $La(OTf)_3$ is too fast to perform the titrations of these, **3** was used as a model for all three phosphates studied in the kinetics. The ${}^{s}_{s}p\mathit{K}_a$ of **3** was determined to be 3.47 ± 0.01 from the average result of the Hyperquad analysis of three separate titrations of 1 × 10^{-3} mol/L **3**, and this value was used in subsequent analyses as a constant. The formation constant for the species $La^{3+}{}_2$:$\mathbf{3}^-$, as a model for the species $La^{3+}{}_2$:$\mathbf{1}^-$, was computed from fitting as were other formation constants for species present in a solution of 2:1 La^{3+}:diphenyl phosphate.

Kinetic measurements

The rate of appearance of *p*-nitrophenol accompanying the methanolysis of **2** was followed by monitoring the increase in absorbance of buffered methanol solutions at 311 nm and 25.0 ± 0.1 °C with a Varian Cary 100 Bio UV–vis spectrophotometer. Its extinction coefficient at 311 nm was determined to be 10 878 ± 479 $(mol/L)^{-1}$ cm^{-1} by averaging the slopes of 17 independent plots of Abs. vs. added [*p*-nitrophenol] over 5 × 10^{-5} mol/L < [La^{3+}] < 1 × 10^{-3} mol/L and 2.5 × 10^{-5} mol/L < [*p*-nitrophenol] < 2.25 × 10^{-4} mol/L. Due to the slow rate of reaction at low [La^{3+}], all reactions

[4] Of course, the kinetics of free-radical-initiated chain reactions such as $H_2 + Br_2 \rightarrow 2HBr$, where the first step requires a dissociation of the Br_2 into 2Br radicals, are well-known to follow a square root dependence in [Br_2] (for a discussion of this mechanism see ref. 6).

in this study were followed to 10% completion and k_{obs} was determined in triplicate using the initial rates method. All reactions were performed at $^{s}_{s}$pH 9.21 ± 0.10 (measured after the kinetic run) using a methanol buffer solution of 1.75 × 10^{-2} mol/L *N*-ethylmorpholine ($^{s}_{s}pK_a$ = 8.60 (measured by half neutralization (3*a*)) partially neutralized with 70% $HClO_4$ (BDH). The solutions prepared in this way contain a small, but kinetically insignificant quantity (<0.1%) of water stemming from that present in the MeOH and what is derived from buffer neutralization. To avoid any chloride ion contamination from the glass electrode that might affect the metal ion reactions, the $^{s}_{s}$pH of the reaction solutions was always determined after kinetic measurements.

To investigate whether the kinetics in the low [La^{3+}] domain result from a 1:1 or a 2:2 La^{3+}:**2**$^{-}$ complex at a given $^{s}_{s}$pH (9.21), it was first necessary to establish the point of transition between the ascending and descending wings of the k_{obs} vs. [La^{3+}] plot (see Fig. 1S, Supplemental information).[3] This kinetic experiment was done using [**2**] = 5 × 10^{-5} mol/L and varying [La^{3+}] between 2.5 × 10^{-5} and 4 × 10^{-3} mol/L; the point of transition was determined to occur at 2 × 10^{-4} mol/L [La^{3+}]. To determine if the kinetically active species was a monomeric 1:1 La^{3+}:phosphate complex or a dimeric 2:2 La^{3+}:phosphate complex, [La^{3+}] and [total phosphate] were varied together such that [total phosphate] = [La^{3+}] = 2 × 10^{-4} to 1.2 × 10^{-3} mol/L. Phosphate **2** had poor solubility in the presence of La^{3+} at concentrations higher than 3 × 10^{-4} mol/L, and so its concentration was held constant at 2 × 10^{-4} mol/L in each case, and the far more soluble phosphate **3** was used make up the [total phosphate] throughout the rest of the concentration range.[5]

Electrospray MS

Mass spectra were determined in methanol using a Waters/Micromass ZQ (Manchester, UK) single quadrupole mass spectrometer equipped with an electospray source operating at cone voltages between 30 and 70 V. The solutions contained [**3**] = 2 × 10^{-4} mol/L, along with equimolar $La(OTf)_3$ and 4 × 10^{-4} mol/L Bu_4NOCH_3, the latter to create **3**$^{-}$ and add 1 equiv. of methoxide to the metal ion. Samples were infused at a flow rate of 10 μL/min; the spectrometer was externally calibrated and run in positive mode.

Results and discussion

The methodology for fitting the kinetic data as a function of varying [La^{3+}] and $^{s}_{s}$pH involves analyzing the speciation of the metal ion alone at low and high concentrations as a function of $^{s}_{s}$pH and then determining the speciation of the phosphate bound forms of the metal ion. All these data can be gleaned from potentiometric titrations under the appropriate conditions. Following analysis of the speciation, one can then fit the kinetic data (Table 1S, Supplemental material)[3] pertaining to k_1**[1]** (the second-order rate constant for La^{3+} promoted methanolysis of **1** at low [La^{3+}] as a function of $^{s}_{s}$pH) and k_2**[1]** (the plateaued pseudo-first-order rate constant for (La^{3+})$_2$:**1**$^{-}$ methanolysis as a function of $^{s}_{s}$pH) as a linear combination of the contribution of various kinetically active species.

Fig. 2. Potentiometric titration data for 0.001 mol/L $La(OTf)_3$ (●), 0.001 mol/L diphenyl phosphate (■), and a mixture of 0.001 mol/L $La(OTf)_3$ and 0.0005 mol/L diphenyl phosphate (▽) determined in methanol at 25 °C.

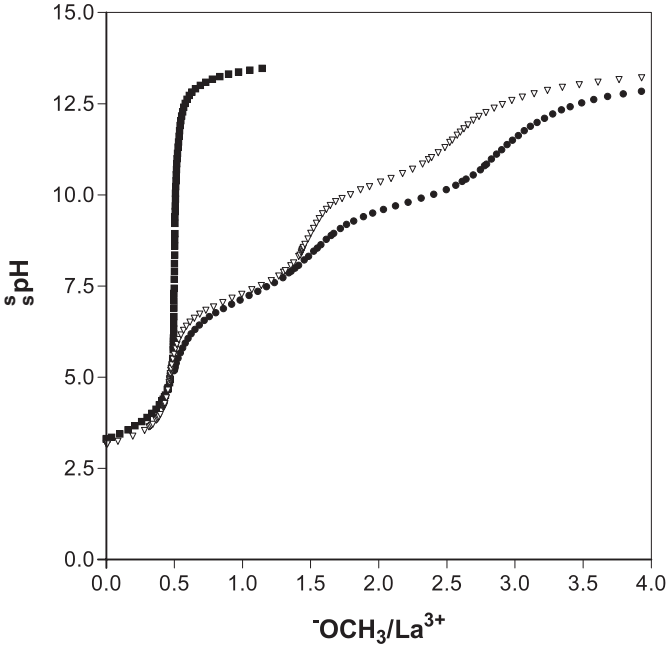

Titration analysis

High [La^{3+}] domain (>10^{-3} mol/L)

In the high [La^{3+}] domain of the k_{obs} vs. [La^{3+}] plots for methanolysis of **1** at each $^{s}_{s}$pH the saturation signifies that the active species comprise two metal ions and one phosphate substrate, the latter most likely bridging the two La^{3+} ions to employ double activation (3*a*, 3*b*). Depending on the $^{s}_{s}$pH, the active (La^{3+})$_2$:**1**$^{-}$ species are also proposed to contain a variable number of methoxides from zero to five (3*a*). The six (La^{3+})$_2$:**1**$^{-}$:($^{-}OCH_3$)$_{0-5}$ forms serve as a starting model to fit the potentiometric titration data for 2:1 La^{2+}:phosphate in methanol at 1 × 10^{-3} mol/L La^{3+}, a concentration within the k_2**[1]** domain. Since **1** is too reactive to survive titration in the presence of La^{3+}, the less reactive phosphate **3** was used in the present study as a structural model. While we recognize that the substitution of **3** for **1** might alter the phosphate binding constants and all formation constants for the associated methoxide containing species, the structural variations should not seriously alter the overall conclusions concerning stoichiometry and formation constants. The titration data for representative titrations of (La^{3+})$_2$:**3**$^{-}$, as well as La^{3+} alone and **3** alone for comparison are illustrated in Fig. 2. The formation constants for the background unbound (La^{3+})$_2$ with one to five methoxides were established first by Hyperquad fitting of a (La^{3+})$_2$($^{-}OCH_3$)$_{1-5}$ model to the titration data for 1 × 10^{-3} mol/L $La(OTf)_3$ in

[5] In previous work (ref. 3*b*) we showed that the effect of a second phosphate diester was to act as a bridge between the two La^{3+} ions to facilitate formation of catalytically active dimers, and that a nonreactive or less-reactive phosphate diester can be used to structurally maximize the formation of active (La^{3+})(reactive phosphate)(surrogate phosphate) dimers.

Table 1. Formation constants for $La^{3+}_2(^-OCH_3)_n$ and La^{3+}_2:**3**$^-$:$(^-OCH_3)_n$ species in methanol at [La^{3+}] = 1×10^{-3} mol/L (25.0 °C).

Equilibrium	$\log {}^{s}_{s}K^{a}$	Microscopic ${}^{s}_{s}pK_a{}^{b}$
$[La_2(^-OCH_3)_1]/[La]^2[^-OCH_3]$	12.79±0.01[c]	
$[La_2(^-OCH_3)_2]/[La]^2[^-OCH_3]^2$	22.33±0.22[c]	${}^{s}_{s}pK_a{}^{2}$ = 7.23±0.21[c]
$[La_2(^-OCH_3)_3]/[La]^2[^-OCH_3]^3$	29.64±0.60[c]	${}^{s}_{s}pK_a{}^{3}$ = 9.46±0.38[c]
$[La_2(^-OCH_3)_4]/[La]^2[^-OCH_3]^4$	36.71±0.39[c]	${}^{s}_{s}pK_a{}^{4}$ = 9.70±0.22[c]
$[La_2(^-OCH_3)_5]/[La]^2[^-OCH_3]^5$	42.68±1.08[c]	${}^{s}_{s}pK_a{}^{5}$ = 10.80±0.69[c]
$[La_2(\mathbf{3}^-)]/[La]^2[\mathbf{3}^-]$	10.47±0.47[d]	
$[La_2(\mathbf{3}^-)(^-OCH_3)_1]/[La]^2[\mathbf{3}^-][^-OCH_3]$	20.15±0.51[d]	${}^{s}_{s}pK_a{}^{1}$ = 7.09±0.04[d]
$[La_2(\mathbf{3}^-)(^-OCH_3)_2]/[La]^2[\mathbf{3}^-][^-OCH_3]^2$	29.48±0.51[d]	${}^{s}_{s}pK_a{}^{2}$ = 7.44±0.01[d]
$[La_2(\mathbf{3}^-)(^-OCH_3)_3]/[La]^2[\mathbf{3}^-][^-OCH_3]^3$	36.12±0.42[d]	${}^{s}_{s}pK_a{}^{3}$ = 10.13±0.10[d]
$[La_2(\mathbf{3}^-)(^-OCH_3)_4]/[La]^2[\mathbf{3}^-][^-OCH_3]^4$	42.32±0.52[d]	${}^{s}_{s}pK_a{}^{4}$ = 10.57±0.11[d]
$[La_2(\mathbf{3}^-)(^-OCH_3)_5]/[La]^2[\mathbf{3}^-][^-OCH_3]^5$	47.07±0.03[d]	${}^{s}_{s}pK_a{}^{5}$ = 12.02±0.50[d]

[a]Derived from fits of the potentiometric titration data using the program Hyperquad (10).
[b]Defined as $-\log {}^{s}_{s}K_a$ for La^{3+}_2:**3**$^-$:$(^-OCH_3)_n(HOCH_3)_x \rightleftharpoons La^{3+}_2$:**3**$^-$:$(^-OCH_3)_{n+1}(HOCH_3)_y + H^+$, calculated from data in column 2 as 16.77 – (${}^{s}_{s}pK_a{}^{n} - {}^{s}_{s}pK_a{}^{n-1}$) where 16.77 is the –log of the autoprotolysis constant for pure methanol.
[c]Averages of duplicate titrations of La(OTf)$_3$ (1×10^{-3} mol/L). Errors are calculated as the standard deviation of the mean.
[d]Averages of duplicate titrations of La(OTf)$_3$ (1×10^{-3} mol/L) in the presence of **3** (5×10^{-4} mol/L). Errors calculated as the standard deviation of the mean.

methanol. In Table 1 are presented the average of the log formation constants (log β or $\log {}^{s}_{s}K$) for three separate determinations that were used as constants for all subsequent analyses of the titrations in the presence of **3**. The ${}^{s}_{s}pK_a$ of **3** (3.47 ± 0.01) was also used as an experimentally determined constant, and the autoprotolysis constant for pure methanol ($10^{-16.77}$) (13) was included as the last constant for the fits. Table 1 shows the results for the formation constants of all the species used as the model in the Hyperquad fitting. The concentrations of the various $(La^{3+})_2$:**1**$^-$:$(^-OCH_3)_{0-5}$ species were subsequently computed as a function of ${}^{s}_{s}pH$ from these formation constants using HySS, another program in the Hyperquad 2000 suite. The speciation diagram shown in Fig. 3 was constructed using conditions relevant to the kinetics where [La^{3+}] = 2×10^{-3} mol/L and [**3**] = 2×10^{-5} mol/L. Also superimposed on Fig. 3 are the kinetic data for k_2**1** in units of s^{-1} from Table 1S[3] (3*a*) as a function of ${}^{s}_{s}pH$ to indicate possible species that may contribute to the rate constant. From the appearance of the latter plot, it is clear that no single species is responsible for the kinetic behaviour, and thus a more detailed analysis is required.

Low [La^{3+}] domain (<2 × 10^{-4} mol/L)

Due to the fact that the overall behaviour is a composite of two independent pathways, we analyze the k_{obs} vs. [La^{3+}] data at the limits of two concentration domains. In the low [La^{3+}] domain, the k_{obs} vs. [La^{3+}] plots for the La^{3+} catalyzed methanolysis of **1** show a linear increase corresponding to an apparent second-order process, with the gradient taken to be k_1**1** in units of $(mol/L)^{-1}\ s^{-1}$. The active form is believed to be a transiently formed La^{3+} bound phosphate, formulated preliminarily as La^{3+}:**1**$^-$:$(^-OCH_3)_n$, where the number of methoxides is zero to two depending on the ${}^{s}_{s}pH$. Since not all the substrate is bound in this region, the apparent second-order kinetics could also be accommodated by the process depicted in eq. [1], where k_1**1** = k_{cat}/K_B ($(mol/L)^{-1}\ s^{-1}$), where k_{cat} refers either to the spontaneous decomposition of La^{3+}:**1**$^-$:$(^-OCH_3)_n$ or to the second-order rate constant for the attack of external methoxide on La^{3+}:**1**$^-$:$(^-OCH_3)_{n-1}$.

Fig. 3. Speciation diagram for La^{3+}_2:**1**$^-$:$(^-OCH_3)_n$ forms as a function of ${}^{s}_{s}pH$ computed from the formation constants given in Table 1 for the titration of diphenyl phosphate (2×10^{-5} mol/L) and 2×10^{-3} mol/L La^{3+}. Captions of 2:1:*n* refer to La^{3+}_2:**1**$^-$:$(^-OCH_3)_n$ forms with a variable number of methoxides, (— — —) La^{3+}_2:**1**$^-$:$(^-OCH_3)_1$, (- - - - -) La^{3+}_2:**1**$^-$:$(^-OCH_3)_3$, (—·—·) La^{3+}_2:**1**$^-$:$(^-OCH_3)_4$. Data superimposed on the figure as (■) are first-order rate constants (k_2) for the La^{3+} catalyzed methanolysis of methyl (4-nitrophenyl) phosphate (**1**) from ref. 3*a*.

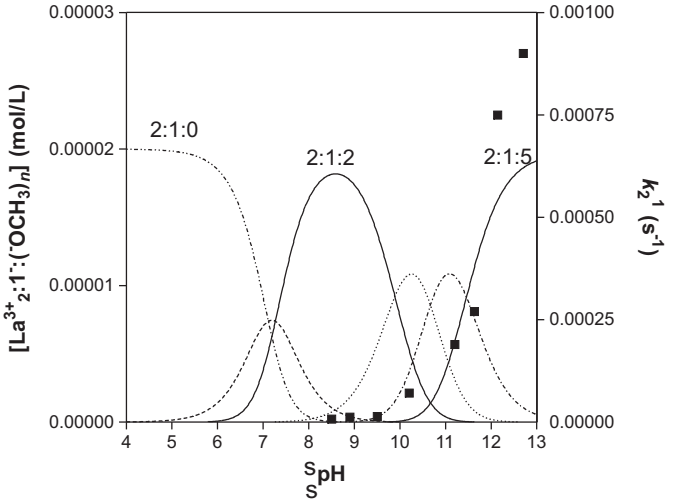

[1] $La^{3+}(^-OCH_3)_n + \mathbf{1}^- \underset{K_B}{\rightleftharpoons} La^{3+}:\mathbf{1}^-:(^-OCH_3)_n \xrightarrow{k_{cat}} P$

There is some ambiguity as to whether the reaction proceeds through the above monomeric form, or through a double

Table 2. Formation constants for various La^{3+} containing species in methanol at $[La^{3+}] = 1 \times 10^{-4}$ mol/L (25.0 °C).

Equilibrium	$\log {}^{s}_{s}K^{a}$	Microscopic ${}^{s}_{s}pK_a{}^{b}$
$[La(^{-}OCH_3)_1]/[La][^{-}OCH_3]$	9.09±0.08[c]	
$[La_2(^{-}OCH_3)_3]/[La]^2[^{-}OCH_3]^3$	28.35±0.38[c]	
$[La_2(^{-}OCH_3)_4]/[La]^2[^{-}OCH_3]^4$	34.66±0.23[c]	${}^{s}_{s}pK_a{}^{3} = 10.45\pm0.61$[c]
$[La_2(^{-}OCH_3)_5]/[La]^2[^{-}OCH_3]^5$	41.55±0.09[c]	${}^{s}_{s}pK_a{}^{4} = 9.88\pm0.32$[c]

[a]Derived from fits of the potentiometric titration data using the program Hyperquad (10).
[b]Defined as $-\log {}^{s}_{s}K_a$ for $La^{3+}(^{-}OCH_3)_n(HOCH_3)_x \rightleftharpoons La^{3+}(^{-}OCH_3)_{n+1}(HOCH_3)_y + H^+$, calculated from data in column 2 as $16.77 - ({}^{s}_{s}pK^{n} - {}^{s}_{s}pK^{n-1})$ where 16.77 is the –log of the autoprotolysis constant for pure methanol.
[c]Averages of duplicate titrations of $La(OTf)_3$ (1×10^{-4} mol/L). Errors are calculated as the standard deviation of the mean.

phosphate bridged dimer formulated as $(La^{3+})_2$:(phosphate^{-})$_2$:$(^{-}OCH_3)_m$ as was determined to be the case in the La^{3+} promoted methanolysis of 2-hydroxypropyl *p*-nitrophenyl phosphate (3*b*). To cast light on this question, two independent sets of experiments were performed. In the first, the electrospray mass spectrum of a methanol solution containing 2×10^{-4} mol/L of both $La^{3+}(^{-}OTf)_3$ and phosphate diester **3** (chosen because it is kinetically stable during the experimental measurement while **1** is not) displayed masses at *m*/*z* 419.12 and 451.15 indicative of La^{3+}:**3**$^{-}$:$(^{-}OCH_3)(HOCH_3)_{0,1}$, but no masses indicative of any dimeric forms. In the second set of experiments, the kinetics for methanolysis of **2** in the presence of equimolar La^{3+} were determined at an initial concentration corresponding to the point of transition (2×10^{-4} mol/L) between the low and high $[La^{3+}]$ domains observed in the k_{obs} vs. $[La^{3+}]$ plot for the methanolysis of **2**. This same trend and point of transition was previously observed in the methanolysis of **1** ((3*a*), see Fig. 1S, Supplemental material).[3] The kinetics of the methanolysis of **2** were then determined as a function of varying $[La^{3+}]$ concentration, but maintaining the $[La^{3+}]$:$[phosphate]_{total}$ ratio at 1.0. Under these conditions, one anticipates shifting a putative 2(La^{3+}:phosphate) $\rightleftharpoons$ (La^{3+}:phosphate)$_2$ equilibrium to the right so that if the dimeric species is active, an increase in observed rate constant, with possible saturation, will accompany the increase in [La^{3+}:phosphate]. This phenomenon was previously observed with the La^{3+} : 2-hydroxypropyl *p*-nitrophenyl phosphate system (3*b*). Above a concentration of 2×10^{-4} mol/L, the complex of phosphate **2** is poorly soluble in this medium so the additional phosphate concentration was made up with the more soluble **3**, but this change will not alter significantly the kinetic result since the observed reaction concerns the decomposition of **2** (2). The k_{obs} for methanolysis of **2** determined under these conditions is invariant to increasing $[La^{3+}]$ within experimental error ($k_{obs} = (2.43 \pm 0.12) \times 10^{-4}$ s^{-1}, Table 2S, Supplemental material)[3] as expected if the reactive species is the monomeric form La^{3+}:**2**: $(^{-}OCH_3)_n$.

Having established that La^{3+} monomers are active in the low $[La^{3+}]$ domain, we turned our attention to the analysis of the titration data in this concentration range. Shown in Fig. 3S, Supplementary material[3] is the titration curve for a 1×10^{-4} mol/L solution of $La(OTf)_3$ in methanol. The general appearance of this curve is quite different from the profile obtained at 1×10^{-3} mol/L (see Fig. 2) in that the first consumption of methoxide follows a regular titration profile consuming 1 equiv. of methoxide per La^{3+} followed by a much steeper profile for the consumption of additional methoxides. The steeper profile corresponding to the addition of more than 1 equiv. of $^{-}OCH_3$ per La^{3+} suggests that dimers or higher order aggregates are formed in that region. Therefore, for the low $[La^{3+}]$ titrations we analyzed the data in terms of a model comprising La^{3+}, $La^{3+}(^{-}OCH_3)_{0,1}$, and $(La^{3+})_2(^{-}OCH_3)_{3,4,5}$. The goodness-of-fit of this model to the titration profile up to ${}^{s}_{s}$pH 11 is shown in Fig. 3S,[3] and in Table 2 are presented the computed formation constants for all the species in this model. These were then used to compute the speciation diagram using HySS for the kinetically relevant conditions where $[La^{3+}] = 1 \times 10^{-4}$ mol/L. This speciation diagram is represented in Fig. 4 along with the overlaid kinetic data that refer to $k_1^{\mathbf{1}}$ in (mol/L)$^{-1}$ s^{-1} for the La^{3+} catalyzed methanolysis of **1** as a function of ${}^{s}_{s}$pH.

Kinetic analysis

High [La^{3+}] domain (>10^{-3} mol/L)

The fits of the titration data to the models previously described provide the concentration of all the participating species as a function of ${}^{s}_{s}$pH in the low and high $[La^{3+}]$ domains. In each domain we can fit the observed rate constants ($k_1^{\mathbf{1}}$ or $k_2^{\mathbf{1}}$) at the various ${}^{s}_{s}$pH values for the La^{3+} catalyzed methanolysis of **1** (3*a*) as linear combinations of the contributions of the individual species. For $k_2^{\mathbf{1}}$ vs. ${}^{s}_{s}$pH in the high $[La^{3+}]$ domain, the appropriate linear combination is given as eq. [2], where each of the $(La^{3+})_2$:**1**$^{-}$:$(^{-}OCH_3)_n$ species contributes its own first-order rate constant ($k_2^{2:\mathbf{1}:n}$) for reaction.

$$[2] \qquad k_2^{\mathbf{1}} = \sum_{n=1}^{5} k_2^{2:\mathbf{1}:n}[(La^{3+})_2:\mathbf{1}^{-}:(^{-}OCH_3)_n]/[\mathbf{1}]_{total}$$

This equation is appropriate for spontaneous breakdown of the substrate-bound species to methanolyzed product via an internal La^{3+} coordinated methoxide mechanism, the transition structure of which is not implied other than it probably contains a dual role for the metal ion as a Lewis acid and deliverer of nucleophilic methoxide. An alternative, and kinetically equivalent, mechanism requires external methoxide attack on the $(La^{3+})_2$:**1**$^{-}$ bound species having one less methoxide than in the internal methoxide model, the appropriate kinetic equation being shown as eq. [3] where

Fig. 4. Speciation diagram for La^{3+} species as a function of $^{s}_{s}$pH computed from the formation constants given in Table 2 for the titration of 1×10^{-4} mol/L La^{3+}. Data superimposed on the figure as (■) are second-order rate constants ($k_1^{\mathbf{1}}$) for the La^{3+} catalyzed methanolysis of methyl (4-nitrophenyl) phosphate (**1**) from ref. 3*a*.

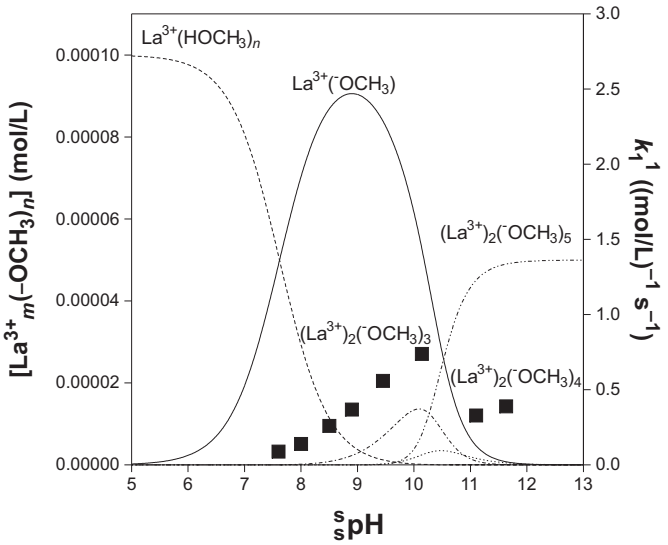

$k'_2{}^{2:\mathbf{1}:n}$ is a second-order rate constant for methoxide attack on each species.

$$[3] \qquad k_2^{\mathbf{1}} = \sum_{n=0}^{4} k'_2{}^{2:\mathbf{1}:n}[(La^{3+})_2:\mathbf{1}^{-}:(^{-}OCH_3)_n][^{-}OCH_3]/[\mathbf{1}]_{total}$$

Given in Table 3 are the rate constants derived from fitting the $k_2^{\mathbf{1}}$ data to eqs. [2] and [3] with the results being displayed in Fig. 5, which includes the individual contributions for all species found to have activity. Their sum generates the overall best fit curve, which is remarkably good given the inherent assumptions of approximating the La^{3+}:**1**$^{-}$ stability constants through the use of **3**. Although the caption for Fig. 5 is specific for the internal methoxide model, the fit is obviously identical for the kinetically equivalent external methoxide model where the $(La^{3+})_2$:**1**$^{-}$:$(^{-}OCH_3)_n$ species responsible for catalysis have one less associated methoxide than in the internal model. The kinetically active forms for the internal methoxide process are $(La^{3+})_2$:**1**$^{-}$:$(^{-}OCH_3)_{2,3,4,5}$, while for the external methoxide process, the reaction is computed to proceed via methoxide attack on $(La^{3+})_2$:**1**$^{-}$:$(^{-}OCH_3)_{1,2,3,4}$.

There is nothing by way of argument that might allow one to prefer one or the other of the described two mechanisms. The computed rate constants for internal methoxide spontaneous decomposition of $(La^{3+})_2$:**1**$^{-}$:$(^{-}OCH_3)_{2,3,4,5}$ are 6.3×10^{-6}, 9.8×10^{-5}, 1.4×10^{-4}, and 1.3×10^{-3} s^{-1}, respectively, consistent with the expectation that the species having the highest basicity for its associated methoxide will react the fastest. For the external methoxide process, the computed second-order rate constants for methoxide on the bound forms with one to four associated methoxides are 1.5×10^4, 3.7×10^2, 2.5×10^2, and 3.3×10^1 $(mol/L)^{-1}$ s^{-1}, respectively, but are well below the limit of ~10^{10} $(mol/L)^{-1}$ s^{-1}, which would be appropriate for a diffusion-limited process involving reaction of an anion and a positively charged species (14). Nevertheless, the rate constants for the external methoxide model are considerably larger than the experimental second-order rate constant for methoxide attack on **1** alone of $(7.9 \pm 0.6) \times 10^{-7}$ $(mol/L)^{-1}$ s^{-1} at 25 °C (3*a*), indicating that complexation of **1** to the $(La^{3+})_2(^{-}OCH_3)_{1,2,3,4}$

Table 3. Computed $k'_2{}^{2:\mathbf{1}:n}$ or $k_2^{2:\mathbf{1}:n}$ rate constants for various species for the La^{3+} catalyzed methanolysis of **1** computed from fits of k_2 vs. $^{s}_{s}$pH data to eq. [2] and [1].

$[La^{3+}{}_2$:**1**$^{-}$:$(^{-}OCH_3)_n]$	$k'_2{}^{2:\mathbf{1}:n}$ or $k_2^{2:\mathbf{1}:n}$
External methoxide model (eq. [3])	
$La^{3+}{}_2$:**1**$^{-}$:$(^{-}OCH_3)_1$	$k'_2{}^{2:\mathbf{1}:1} = (1.5\pm0.2)\times10^{4}$[a]
$La^{3+}{}_2$:**1**$^{-}$:$(^{-}OCH_3)_2$	$k'_2{}^{2:\mathbf{1}:2} = (3.7\pm0.6)\times10^{2}$[a]
$La^{3+}{}_2$:**1**$^{-}$:$(^{-}OCH_3)_3$	$k'_2{}^{2:\mathbf{1}:3} = (2.5\pm0.4)\times10^{2}$[a]
$La^{3+}{}_2$:**1**$^{-}$:$(^{-}OCH_3)_4$	$k'_2{}^{2:\mathbf{1}:4} = (3.3\pm0.5)\times10^{1}$[a]
Internal methoxide model (eq. [2])	
$La^{3+}{}_2$:**1**$^{-}$:$(^{-}OCH_3)_2$	$k_2^{2:\mathbf{1}:2} = (6.3\pm0.9)\times10^{-6}$[b]
$La^{3+}{}_2$:**1**$^{-}$:$(^{-}OCH_3)_3$	$k_2^{2:\mathbf{1}:3} = (9.8\pm1.5)\times10^{-5}$[b]
$La^{3+}{}_2$:**1**$^{-}$:$(^{-}OCH_3)_4$	$k_2^{2:\mathbf{1}:4} = (1.4\pm0.2)\times10^{-4}$[b]
$La^{3+}{}_2$:**1**$^{-}$:$(^{-}OCH_3)_5$	$k_2^{2:\mathbf{1}:5} = (1.3\pm0.2)\times10^{-3}$[b]

Note: Errors computed from the avg. % deviation in the fitted numbers calculated by eq. [2] or [3] from the actual kinetic data. Data fit under the assumption that the various La^{3+}:**3**$^{-}$:$(^{-}OCH_3)_n$ formation constants from Table 1 are realistic approximations for those for the La^{3+}:**1**$^{-}$:$(^{-}OCH_3)$ system.

[a]Values of $k'_2{}^{2:\mathbf{1}:n}$ are actually second-order rate constants in units of $(mol/L)^{-1}$ s^{-1} after accounting for the $^{-}OCH_3$ concentration.

[b]Values of $k_2^{2:\mathbf{1}:n}$ in units of s^{-1}.

Fig. 5. Plot of $k_2^{\mathbf{1}}$ vs. $^{s}_{s}$pH for the $La^{3+}{}_2$ catalyzed methanolysis of **1** and the contributionsof each active species. Lines come from the fit of the kinetic data to eq. [2]. Solid line, composite of all contributions; (—••—••), contribution of $La^{3+}{}_2$(**1**$^{-}$)$(^{-}OCH_3)_2$; (— — —), contribution of $La^{3+}{}_2$(**1**$^{-}$)$(^{-}OCH_3)_3$; (•••), contribution of $La^{3+}{}_2$(**1**$^{-}$)$(^{-}OCH_3)_4$; (—•—•), contribution of $La^{3+}{}_2$(**1**$^{-}$)$(^{-}OCH_3)_5$.

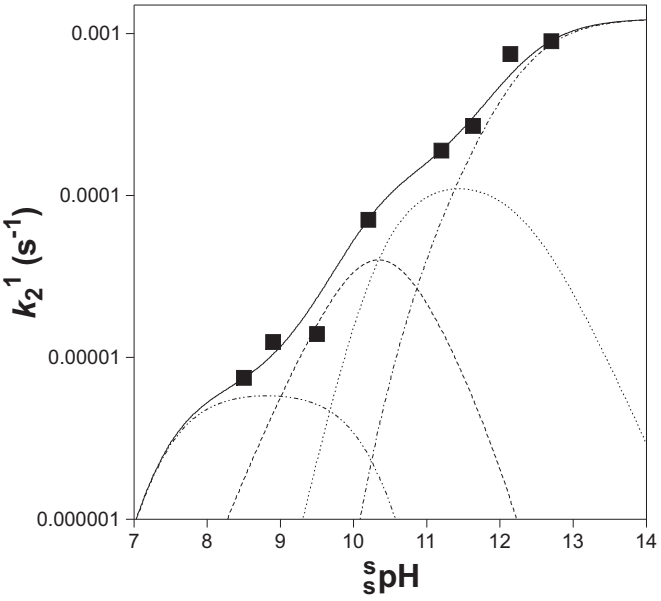

system provides a catalytic enhancement varying from 1.9×10^{10}-fold to 4×10^7-fold, with the least catalysis being observed for methoxide attack on the least positively charged complex.

Low [La^{3+}] domain

As stated previously, in the low [La^{3+}] domain the kinetics are linearly dependent on the metal ion. Thus, the preferred fitting procedure considers that the $k_1^{\mathbf{1}}$ rate constants at each $^{s}_{s}$pH can be described as a linear combination of second-order rate constants (equivalent to k_{cat}/K_B at each $^{s}_{s}$pH) for each of the contributing $(La^{3+})(^{-}OCH_3)_n$ species for the internal methoxide model. For the external methoxide model (eq. [4]), the rate constants are now third-order to accommodate the methoxide concentration that has been factored out.

At low [La^{3+}] the only monomeric species available in solution, as revealed by fits of the potentiometric curve, are $La^{3+}(^{-}OCH_3)_{0,1}$ and it immediately becomes clear that: (1) each species is required to provide a satisfactory fit to the kinetic $k_1^{\mathbf{1}}$ data; and (2) that an additional methoxide is required to explain the activity seen where $La^{3+}(^{-}OCH_3)_1$ is the dominant species to accommodate the increase in rate with $^{s}_{s}$pH. Thus, the internal methoxide mechanism is rendered unlikely because, if operative, the kinetic data would have to track the concentration behaviour of $La^{3+}(^{-}OCH_3)_1$ as a function of $^{s}_{s}$pH, which it does not: correspondingly, the external methoxide mechanism is favoured. Given in Table 4 are the best-fit rate constants from the application of eq. [4], which generate the species contributions to the overall fitted curve presented in Fig. 6 for $k_1^{\mathbf{1}}$ as a function of $^{s}_{s}$pH. The overall fit displayed in Fig. 6, while not as good as obtained for the $k_2^{\mathbf{1}}$ data vs. the $(La^{3+})_2$:$\mathbf{1}^{-}$:$(^{-}OCH_3)_n$ species, is still considered satisfactory in view of the inherent errors in determining the linear region of the k_{obs} vs. $^{s}_{s}$pH profile and the assumed speciation to fit the titration data. The computed constants of 3×10^8 and 5.1×10^6 $(mol/L)^{-2}$ s^{-1} refer to the apparent termolecular processes corresponding to CH_3O^{-} + $\mathbf{1}^{-}$ + $La^{3+}(^{-}OCH_3)_{0,1}$ respectively, the reduction by a factor of ~60-fold in rate constant between the two resulting from Lewis acidity differences attributable to the methoxide content of the respective complexes.

$$[4] \qquad k_1^{\mathbf{1}} = \sum_{n=0}^{1} k_1'^{1:n}[La^{3+}(^{-}OCH_3)_n][^{-}OCH_3]/[La^{3+}]_{total}$$

While the fitting provides the apparent third-order rate constant for the process involving CH_3O^{-} + $\mathbf{1}^{-}$ + $La^{3+}(^{-}OCH_3)_{0,1}$, it is difficult to envision any mechanism where there is not a preequilibrium binding of the substrate to the metal ion followed by attack of methoxide on that complex as in eq. [1]. On the basis of the experimental kinetic saturation plots of k_{obs} vs. [La^{3+}] (3*a*), we estimate the complex between an oppositely charged phosphate and metal ion to have a dissociation constant (K_{dis}) between 2×10^{-4} and 10^{-3} mol/L depending on the metal ion charge as controlled by the number of metal bound methoxides (n = 0, 1). Accordingly, one can calculate the second-order rate constant for methoxide attack on the transiently bound substrate as being between 6×10^4 and 3×10^5 $(mol/L)^{-1}$ s^{-1} in the case of the complex with n = 0, and 10^3 to 5×10^3 $(mol/L)^{-1}$ s^{-1} for the attack of methoxide on the complex with n = 1. Relative to the experimental second-order rate constant for methoxide attack on $\mathbf{1}^{-}$ alone of $(7.9 \pm 0.6) \times 10^{-7}$ $(mol/L)^{-1}$ s^{-1} at 25 °C (3*a*), coordination to $La^{3+}(^{-}OCH_3)_{0,1}$ provides a rate enhancement of at least 10^{11}- to 10^9-fold depending on the overall charge of the metal:substrate complex.

Table 4. Computed $k'^{1:n}_1$ or $k_1^{1:n}$ rate constants for various species for the La^{3+} catalyzed methanolysis of **1** computed from fits of $k_1^{\mathbf{1}}$ vs. $^{s}_{s}$pH data to eq. [4].

$[La^{3+}(^{-}OCH_3)_n]$	$k'^{1:n}_1$
External methoxide model (eq. [4])	
$La^{3+}(^{-}OCH_3)_0$	$k'^{1:0}_1 = (3.0\pm0.6)\times10^{8a}$
$La^{3+}(^{-}OCH_3)_1$	$k'^{1:1}_1 = (5.1\pm0.9)\times10^{6a}$

Note: Errors computed from the avg. % deviation in the fitted numbers calculated by eq. [4] from the actual kinetic data.

[a]Values of $k'^{1:n}_1$ are third-order rate constants in units of $(mol/L)^{-2}$ s^{-1} after accounting for the $^{-}OCH_3$ concentration.

Fig. 6. Plot of $k_1^{\mathbf{1}}$ vs. $^{s}_{s}$pH for the La^{3+} catalyzed methanolysis of **1** and the contributions of each active species. Lines come from the fit of the kinetic data to the external methoxide model given in eq. [4]. Solid line, composite of all contributions; (— — —), contribution of $La^{3+}(^{-}OCH_3)_0$; (···), contribution of $La^{3+}(^{-}OCH_3)_1$.

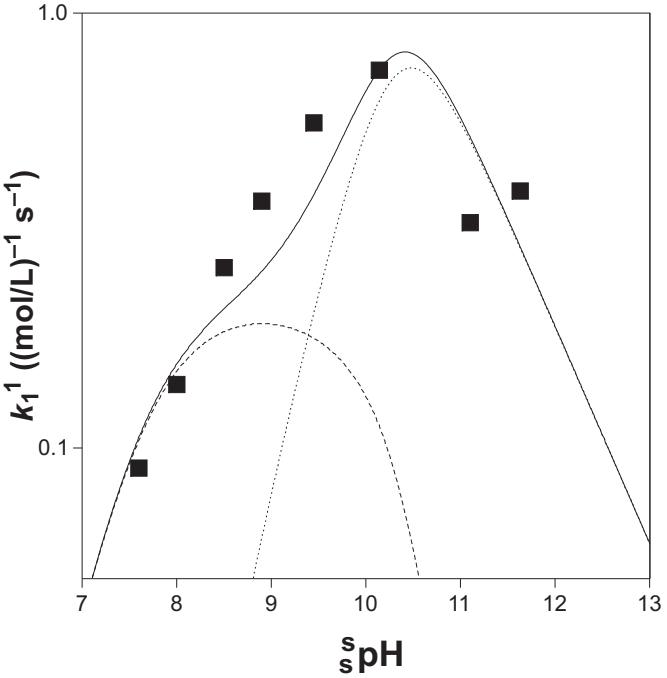

Conclusions

In this paper we have presented a detailed analysis of the kinetic contributions of various La^{3+} species catalyzing the methanolysis of the phosphate diester **1** for which kinetic data were presented previously (3*a*), but only qualitatively analyzed within the framework of Scheme 1. By coupling the rate data to an analysis of the speciation of the La^{3+} containing complexes present in solution as a function of $^{s}_{s}$pH one can provide a simplified, but satisfactory, model to explain the kinetic behaviour in the high and low [La^{3+}] domains. We anticipate that such an approach will prove

beneficial to explain the origins of nonunit, or irregular dependencies of kinetic profiles of many other metal-ion-catalyzed reactions where the metal ion undergoes changes in speciation as a function of $^{s}_{s}$pH.

There is an interesting observation revealed by comparing these analyses with those previously reported for the La^{3+} promoted catalysis of the methanolysis of neutral substrates such as phosphate triesters (3*c*, 3*d*) and carboxylate esters (1). In those cases, the pH/rate profiles are bell-shaped or distorted bell-shaped and best accommodated by mechanisms involving a dual role for the metal ion as a Lewis acid and deliverer of a metal-coordinated methoxide on a transiently bound neutral substrate. However, in the present cases where there is stronger binding of the anionic phosphate to the metal ion to produce a thermodynamically more stable complex, the pH/rate profiles for both the La^{3+} monomer and dimer cases show gradual increases with non-integral slopes. The preferred analysis involves attack of external methoxide on the relatively stable complex where the main apparent role of the metal ion is to act as a Lewis acid or electrostatic stabilizer of the developing negative charge in the TS. While we offer no detailed explanation of the difference in behaviour between neutral and anionic substrates at this time, it must be related to a counterbalancing of the effects of coordination geometry, Lewis acid activation, relative nucleophilicity of metal-bound and external nucleophiles, and geometry of the activated complexes for each mode of catalysis.

Acknowledgements

The authors gratefully acknowledge the financial assistance of Queen's University and the Natural Sciences and Engineering Research Council of Canada (NSERC) to which G.T.T. Gibson is particularly thankful for the award of a Canada Graduate Scholarship–D. A.C.T. Teng is also indebted to NSERC for the award of an Undergraduate Summer Research Award.

References

1. (*a*) A.A. Neverov, T. McDonald, G. Gibson, and R.S. Brown. Can. J. Chem. **79**, 1704 (2001); (*b*) A.A. Neverov, N.E. Sunderland, and R.S. Brown. Org. Biomol. Chem. **3**, 65 (2005).
2. P.J. Montoya-Pelaez, G.T.T. Gibson, A.A. Neverov, and R.S. Brown. Inorg. Chem. **42**, 8624 (2003).
3. (*a*) A.A. Neverov and R.S. Brown. Inorg. Chem. **40**, 3588 (2001); (*b*) J.S.W. Tsang, A.A. Neverov, and R.S. Brown. J. Am. Chem. Soc. **125**, 1559 (2003); (*c*) J.S.W. Tsang, A.A. Neverov, and R.S. Brown. Org. Biomol. Chem. **2**, 3457 (2004); (*d*) J.S. Tsang, A.A. Neverov, and R.S. Brown. J. Am. Chem. Soc. **125**, 7602 (2003).
4. (*a*) J.F. Davies, Z. Hostomska, Z. Hostomsky, S.R. Jordan, and D.A. Mathews. Science (Washington, D.C.), **252**, 88 (1991); (*b*) L.S. Beese and T.A. Steitz. EMBO J. **10**, 25 (1991); (*c*) A. Lahm, S. Volbeda, and D. Suck. J. Mol. Biol. **215**, 207 (1990).
5. R.S. Brown and A.A. Neverov. J. Chem. Soc. Perkin Trans. 2, 1039 (2002), and refs. 2 and 31 therein.
6. A.A. Frost and R.G. Pearson. Kinetics and mechanism: A study of homogeneous chemical reactions. 2nd ed. John Wiley and Sons, New York. 1965. pp. 236–261.
7. W. Desloges, A.A. Neverov, and R.S. Brown. Inorg. Chem. **43**, 6752 (2004).
8. (*a*) J.R. Morrow and W.C. Trogler. Inorg. Chem. **28**, 2330 (1988); (*b*) (erratum to ref. 8*a*): J.R. Morrow and W.C. Trogler. Inorg. Chem. **31**, 1544 (1992).
9. J. Suh and S.H. Hong. J. Am. Chem. Soc. **120**, 12 545 (1998).
10. Hyperquad 2000 is a computer program that applies nonlinear curve fitting to a titration by adjusting a series of formation constants (log β) for species input to a model, published in: P. Gans, A. Sabatini, and A. Vacca. Talanta, **43**, 1739 (1996).
11. G. Gibson, A.A. Neverov, and R.S. Brown. Can. J. Chem. **81**, 495 (2003).
12. (*a*) C.L. deLigny and M. Rehbach. Recl. Trav. Chim. **79**, 727 (1960); (*b*) R.G. Bates, M. Paabo, and R.A. Robinson. J. Phys. Chem. **67**, 1833 (1963); (*c*) R.G. Bates. Determination of pH: Theory and practice. 2nd ed. John Wiley and Sons, New York. 1964. p. 245.
13. (*a*) I. Canals, J.A. Portal, E. Bosch, and M. Rosés. Anal. Chem. **72**, 1802 (2000); (*b*) E. Bosch, F. Rived, M. Roses, and J. Sales. J. Chem. Soc. Perkin Trans. 2, 1953 (1999); (*c*) F. Rived, M. Rosés, and E. Bosch. Anal. Chim. Acta, **374**, 309 (1998); (*d*) E. Bosch, P. Bou, H. Allemann, and M. Roses. Anal. Chem. **68**, 3651 (1996).
14. (*a*) A. Fersht. Enzyme structure and mechanism. W.H. Freeman and Co., New York. 1985. pp. 147 to 148; (*b*) M. Eigen and L.Z. De Maeyer. Electrochemistry, **59**, 986 (1955).